

1 **Online Integrated Fractionation-Hydrolysis of Lignocellulosic**
2 **Biomass using Sub- and Supercritical Water**

3
4 Cristian M. Piqueras¹, Álvaro Cabeza², Gianluca Gallina², Danilo A. Cantero², Juan
5 García-Serna^{2*} and María J. Cocero²

6
7 ¹Planta Piloto de Ingeniería Química, PLAPIQUI-Universidad Nacional del Sur-
8 CONICET, Camino La Carrindanga km 7-CC 717, (8000) Bahía Blanca, Argentina.

9 Phone: +542914861700 / Fax:+542914871600

10 ²High Pressure Processes Group, Department of Chemical Engineering and
11 Environmental Technology, University of Valladolid, Escuela de Ingenierías
12 Industriales, (47011) Valladolid, Spain. Phone: +34 983184934

13 *e-mail address: jgserna@iq.uva.es

14
15
16 **Keywords:** Glucose, Glycolaldehyde, Kinetics, Process Development, Xylose, Holm
17 Oak Wood

18

19 **Abstract**

20 A novel process coupling the fractionation and hydrolysis reactors is presented. Holm oak was
21 used as real lignocellulosic biomass to be treated. In the fractionation reactor, hemicellulose and
22 cellulose were solubilized and partially hydrolyzed in different stages with the aim of feeding
23 the hydrolysis reactor with high C5 concentrations or C6 concentrations. The fractionation was
24 performed in two stages: at 180°C optimizing the hemicellulose extraction and at 260°C
25 extracting cellulose and hard hemicellulose remaining in the biomass structure. Three water
26 flows were tested: 11, 17 and 26 cm³/min. Sugar yields from 71 to 75% were reached, mainly
27 composed of xylose and glucose oligomers and lower amounts of other chemicals, like retro-
28 aldol products, acetic acid or 5-HMF. The outlet stream from the fractionation reactor was
29 directly mixed with sub or supercritical water at the inlet mixer of a SHR where the reaction
30 time was precisely controlled. The temperature, pressure and reaction time were modified to get
31 an insight of their effect on the yield of retro-aldol condensation products. Yields of 24% for
32 glycolaldehyde, and pyruvaldehyde were found at 8.3 s, 350°C and 162 bar (hydrolysis reactor
33 conditions). In other hand, 25% of lactic acid was found at 0.23 s, 396°C and 245 bar. A
34 discussion based on a known reaction pathway is proposed. Moreover, a kinetic model for the
35 hydrolysis reactor was proposed, being able to reproduce the experimental data with deviations
36 lower than 10 % for sugars and other products extracted. This combined process performs a
37 selective valorization of real lignocellulosic biomass, avoiding the costly process of extreme
38 grinding needed for the fluidization in a continuous hydrothermal process.

39

40 **Introduction**

41 Even if it is reasonably assumed that biomass from plants will be the main carbon source in the
42 future, the choice of which reaction medium should be used to depolymerize and valorize
43 biomass has not been taken yet. Pressurized fluids, especially sub and supercritical water
44 ($T_c=374^\circ\text{C}$ and $P_c= 221$ bar), can be pointed as a promising alternative to depolymerize and
45 valorize biomass [1-5]. Physical and chemical properties of water can be modified by adjusting
46 pressure and temperature around the critical point, making water a reaction medium able to
47 favor different kind of reactions [1]. Because of this reason, hot pressurized water has been used
48 as reaction medium for fractionation [6-9] , hydrolysis [10-12] and valorization of biomass [13-
49 16].

50 The composition of lignocellulosic biomass is highly dependent on the plant species and
51 growth conditions. However, it can be considered that the average composition of
52 lignocellulosic biomass is approximately: cellulose (40% wt.), hemicellulose (25% wt.), lignin
53 (25% wt.), extractives and ashes (10% wt.) [17]. Although biomass is composed by diverse and
54 complex molecules, it can be fractionated principally into C6 sugars (mainly glucose), C5
55 sugars (mainly xylose) and lignin [3]. These three fractions can be further modified to produce a
56 wide range of products like: ethanol, hydrogen, glycolaldehyde, pyruvaldehyde, lactic acid and
57 5-HMF among others [3, 18-25].

58 The fractionation of biomass can be defined as the selective separation of C5 sugars, C6 sugars
59 and lignin from the original biomass matrix. This process was studied under hydrothermal
60 conditions in different ways of operation: batch, semi batch and continuous [3, 26]. Semi batch
61 and continuous processes allow obtaining higher yields of sugars and chemical compounds than
62 batch reactors, because it is possible to control the temperature (T) and the residence time (t_r)
63 more accurately than in batch processes [27]. Continuous processes are the most appropriate to
64 control the reaction conditions (T and t_r), however, in most cases it is necessary to apply
65 expensive pretreatments to the raw material before the fractionation+hydrolysis process, for
66 example: exhaustive size reduction [28]. On the other hand, the continuous process can be

67 performed at different operating conditions in order to separate the C5 sugars from the C6
68 sugars.

69 The extraction of hemicellulose from woody biomass can be carried out at temperatures
70 between 130°C and 260°C, solid reaction times between 20 and 60 min and liquid residence
71 times inside the reactor between 0.1 min and 1 min. At those conditions, hemicellulose can be
72 both extracted and hydrolyzed [29, 30]. After the extraction at 180°C, two products are usually
73 obtained: a liquid composed mainly of C5 sugars and a solid composed of C6 sugars and lignin.
74 These two products can be separated by filtration. Then, the cellulose in the solid can be
75 hydrolyzed at supercritical conditions to obtain a water solution of C6 sugars and a solid
76 enriched in lignin. These processes can be carried out in two reactors with a filtration operation
77 between them. Another option which allows the intensification of the process is using one fixed
78 bed reactor. In such a case, the biomass is loaded in the reactor and the hydrolysis temperature
79 is changed in order to hydrolyze C5 or C6 sugars [31]. The semi batch process allows high
80 performances on the yields of C5 sugars hydrolysis. However, when the reaction temperature is
81 increased to hydrolyze the recalcitrant cellulose and hemicellulose, the yield of recovered sugars
82 decreases because of the increment of the sugars further reactions [10, 11, 32].

83 The continuous reactors have been employed in many applications for the valorization of sugar
84 streams allowing a precise control over the reactions [19-21]. These reactions can be managed
85 using pressurized water and choosing the adequate reaction conditions. For example, at
86 temperatures between 200°C and 300°C (250 bar) the water molecules are highly dissociated
87 favoring the ionic reactions, like the production of 5-HMF from fructose and glucose [1]. On the
88 other hand, at 400°C (250 bar) the water molecules are highly associated favoring the non-ionic
89 reactions, like the retro aldol condensation reactions [1].

90 In this article, a novel integrated fractionation-valorization process was designed and built using
91 wooden biomass as raw material and water (subcritical and supercritical) as reaction medium.
92 The wooden biomass was fractionated in a fixed bed reactor at different temperatures. The
93 solubilized products were directly injected to a continuous near critical water reactor to

94 efficiently convert C5 and C6 sugars into valuable products, like glycolaldehyde,
95 pyruvaldehyde and lactic acid avoiding a further hydrolysis to organic acids. In addition, a
96 kinetic analysis of the biomass hydrolysis was done in order to study the differences in the
97 process when subcritical and supercritical conditions were used.

98 The objective of this research paper was to design a novel process capable of converting
99 lignocellulosic biomass into valuable products eluding the excessive milling of biomass and
100 decreasing the number of reactors.

101

102 **1. Experimental**

103 *2.1 Materials*

104 Deionized water produced by Elix[®] Advantage purification system was used as reaction
105 medium to run the experiments. The standards used in a High Performance Liquid
106 Chromatography (HPLC) analysis were: cellobiose ($\geq 98\%$), glucose ($\geq 99\%$), xylose ($\geq 99\%$),
107 galactose ($\geq 99\%$), mannose ($\geq 99\%$), arabinose ($\geq 99\%$), glyceraldehyde ($\geq 95\%$), glycolaldehyde
108 dimer ($\geq 99\%$), lactic acid ($\geq 85\%$), formic acid ($\geq 98\%$), acetic acid ($\geq 99\%$), acrylic acid ($\geq 99\%$),
109 furfural (99%) and 5-hydroxymethylfurfural ($\geq 99\%$) purchased from Sigma. 0.01 N solution of
110 sulfuric acid (HPLC grade) in Milli-Q[®] grade water was used as the mobile phase in the HPLC
111 analysis. Sulfuric acid ($\geq 96\%$) and calcium carbonate ($\geq 99\%$) supplied by Panreac, Spain, were
112 used as reagents for the quantification procedure of structural carbohydrates and lignin [33].
113 Also, Milli-Q[®] water was used in this determination. Holm oak wood employed as raw material
114 was collected in Spanish forests. The wood was milled obtaining chips with average width of 2
115 mm and average length of 5 mm, as it is shown in Figure S1 of Supplementary Material.

116 *2.2 Analytical methods*

117 The composition of the holm oak wood raw material, exhausted solid and extracted liquor was
118 determined through two Laboratory Analytical Procedures (LAP) from NREL [33, 34]. The
119 procedure for solid samples consists in quantifying the structural carbohydrates and lignin in the
120 biomass as follows. A) The biomass was weighted before and after being dried in an air driven
121 oven at 105 °C for 24 hours in order to calculate the moisture content. B) Dried biomass was

122 treated in a Soxhlet equipment with n-hexane, leaving a solid free of oils and other extractives.
123 C) 300 mg of dried and free-extractives solid from step (b) were hydrolyzed in 3 ml of 72% wt
124 sulfuric acid solution at 30 °C for 30 min, in order to break the bonds between biopolymers and
125 the main solid structure. D) The mixture of oligomers obtained in step (c) is diluted using 84 ml
126 of deionized water and heated at 120 °C for 60 min with the aim of hydrolyzing hemicellulose
127 and cellulose to obtain their correspondent monomers [35]. E) The solid is separated from the
128 solution by vacuum filtration. F) The total mass of solubilized sugars was quantified as the
129 difference in weight between the original solid and the exhausted solid after oven drying at 105
130 °C in oven for 24 hours. G) The exhausted solid is placed in a muffle at 550 °C for 24 h and the
131 remaining residue was weighted before and after this step to calculate the insoluble lignin and
132 the ash content of the sample. H) A liquid aliquot was analyzed with UV-Vis spectrophotometer
133 at 320 nm with extinction coefficient of $34 \text{ Lg}^{-1}\text{cm}^{-1}$ [36] to calculate the amount of soluble
134 lignin. I) Another liquid aliquot was neutralized to pH range 6 to 7, then it was filtered using a
135 0.2 μm membrane and analyzed by HPLC determining the carbohydrates composition. This
136 procedure is performed using a column SUGAR SH-1011 (Shodex) with a 0.01 N of sulfuric
137 acid solution as a mobile phase. To identify the soluble products, two detectors were used:
138 Waters IR detector 2414 (210 nm) and Waters dual λ absorbance detector 2487 (254 nm). In
139 order to calculate the amount of carbohydrates, each chromatogram was integrated numerically
140 by decomposing it into a sum of 9 to 13 Gaussian peaks, minimizing chi squared function of a
141 Levenberg-Marquardt-Flecher algorithm [37]. Glycolaldehyde and Pyruvaldehyde resulted to be
142 overlapped, since the retention time of their standards is extremely close (11.99 vs 12.24
143 minutes, respectively). So we refer to them as glycolaldehyde-pyruvaldehyde.

144 The raw material contained 1.6 % wt. extractives, 1.8% wt. moisture, 0.2% wt. ashes, 24.2% wt.
145 Klason lignin (from which 4.0% corresponds to soluble lignin), 45.7% wt. of hexoses, 23.9%
146 wt. pentoses. The sum of all the components represents the 97.4% of total weight, the
147 discrepancy is due to experimental errors like the loss of solid material after the recovery at the
148 end of the experiments, or the inhomogeneity of the material which can have slightly different

149 compositions depending on the analyzed aliquot; in any case, it is inside the acceptable
150 experimental error.

151 The amount of C6 was calculated as the sum of glucose, cellobiose and fructose concentrations.
152 Xylose was the only C5 detected. Acetic acid was considered to come from the deacetylation of
153 xylan during the extraction process or, as explained in the next sections, from the hydrolysis of
154 pyruvaldehyde. The hydrolysis products from hexoses and pentoses were mainly
155 glyceraldehyde, glycolaldehyde, pyruvaldehyde, lactic acid, 5-hydroxymethylfurfural and in
156 some cases acrylic acid were detected in very low concentration.

157 The procedure followed to analyze liquid samples consists in the steps (C), (D) and (I)
158 described above. In this case, the carbon content liquid solutions was determined by total
159 organic carbon (TOC) analysis using a Shimadzu TOC-VCSH equipment. Every sample was
160 previously filtered using a 0.2 μm syringe filter and diluted 1:10 times with Millipore water.

161 The pH of the outlet stream was measured online using an electronic pH-meter (Nahita model
162 903).

163 *2.3 Experimental setup and operation procedure*

164 The setup used in this work is shown in Figure 1. The system consisted in two reactors online
165 integrated: 1) the fractionation reactor (R.1), where the C5 and C6 are solubilized and partially
166 hydrolyzed; 2) the supercritical hydrolysis reactor (SHR), which converts the soluble
167 compounds into added value products. The fractionation line is composed of a water deposit
168 (D.1), downstream an American Lewa EK6 2KN high pressure pump (P.1, maximum flow rate
169 1.5 kg/h) propels water through a pre-heater (H.1, 200 cm of 1/8" SS 316 pipe, electrically
170 heated by means of two resistors of 300 W) which ensures an uniform temperature at the reactor
171 inlet. The reactor (R.1), a tube of SS 316, 40 cm length, 1.27 cm O.D., is heated by three flat
172 resistors of 300 W each, placed axially along a machined aluminum bar with 5.08 cm O.D.
173 Both, preheater and the reactor are located inside a former chromatographic oven HP5680. The
174 out-flow stream from the extraction line is mixed with the supercritical water stream, entering in
175 a second reactor (SHR) (R.2). The supercritical water line is composed of a heater (H.2), a tube
176 of 18 m, 1/8 in O.D. SS316 wrapped around a brass cylinder and heated by two cartridges and

177 two flat resistors, which provided adjustable power of up to 10 kW, in order to control the
178 temperature of this stream. The water flow was generated by a Milton Roy XT membrane pump
179 (P.2, maximum flow rate 6 kg/h). The SHR allows a fast heating of the biomass stream, which
180 is mixed almost instantaneously with the supercritical water stream, and a rapid cooling of the
181 products, which takes place through a sudden expansion which efficiently stops the hydrolysis.
182 In this way, the reaction time could be precisely calculated, as the reactor works isothermally.
183 Pressure was controlled Micro Metering valve 30VRMM4812 from Autoclave Engineering
184 (V.4). The setups of the two reactors were presented in detail in previous works [32, 38].
185 An average amount of 6.12 ± 0.03 gr of holm oak biomass was placed inside the reactor R.1 for
186 each experiment. Two metallic filters were used (pore diameter ≈ 200 μm), located on the top
187 and bottom of the reactor, avoiding the release of the solid during the experiments. A pressure
188 test with cold pressurized water was carried out before every experiment, with the aim to check
189 the presence of leaks in the system. Then, the supercritical line was heated ensuring the
190 functioning of the system at required operating conditions. Once these conditions were stable,
191 the pumps were switched off and both, the preheater and the reactor R.1, were heated up until
192 the temperatures reached the respective set values. Afterwards, both pumps were switch on
193 again and the flow and pressure were set to the desired conditions, zero time is considered when
194 pressure reached the desired value.

195 A total of 11 experiments were performed (3 fractionations and 8 coupled reactions), obtaining
196 a total of 130 liquid and 11 solid samples, characterized with the methods described above. Six
197 experiments were performed varying the temperature in the SHR from subcritical (350°C) up to
198 supercritical (400°C) conditions, maintaining the pressure at 250 ± 10 bar. The reaction time in
199 this reactor was modified by varying the water flow-rate and changing the reactor volume (2.2
200 or 12.4 cm^3); reaction times between 0.25 s and to 12 s were tested. Three different water flows
201 (11, 17, 26 cm^3/min) were tested in the fractionation line, maintaining constant the ratio with the
202 flow of supercritical water stream, to get the desired conditions during the further hydrolysis.
203 The feed composition to the SHR was analyzed by carrying out three fractionations without the

204 second hydrolysis stage, at the same conditions of temperatures, flow-rates and pressure tested
205 with the coupled reaction.

206 The fractionation in the fixed bed reactor was performed in two stages marked by two distinct
207 temperatures: 180°C to extract the hemicellulose and 260°C to remove most of the cellulose
208 fraction from the biomass. The heating time between both setpoints was in the range of 5-10
209 min, while the flow was temporarily stopped for the experiment running at 26 cm³/min. In order
210 to follow the reaction evolution, the pH of the outlet stream was measured online sampling
211 every 1 minute. Liquid samples (30-40 cm³) were taken according the pH variations every 5 to
212 20 min for the experiment at 11 cm³/min, and every 2 to 8 min for the other experiments. The
213 overall experiment time varied from 110, 60 and 45 min for the runs at 11, 17, 26 cm³/min,
214 respectively (called here as (1), (2) and (3)). After the last sample was grabbed, the heating was
215 turned off and the reactor R.1 was let to cool down to room temperature with air flux. Both
216 pumps were set to zero flow and the system was depressurized. The solid was removed from the
217 reactor, filtered and dried 24 h at 105°C for further analysis. After cleaning, the fixed bed
218 reactor was placed back, tightened and the system was washed out with deionized water.

219

220 **3. Results and Discussion**

221 *3.1. Biomass fractionation*

222 From the analysis of the raw holm oak, the amount of soluble material was $4.65 \pm 0.03\text{g}$,
223 corresponding to 72.1% of the biomass weight. $3.02 \pm 0.02\text{g}$ of this soluble mass were
224 composed of hexoses (C6) and $1.58 \pm 0.01\text{g}$ of pentoses (C5). The spatial time of the liquid (τ_l),
225 is determined using the liquid flow rate, the reactor volume and the average porosity of the bed
226 ($\varepsilon_{i0}=0.457\pm0.01$, $\varepsilon_f=0.948\pm0.019$). The latter was calculated by means of Eq. (1), taking into
227 account the initial and the final fraction of void volume in the bed, due to the shrinking size of
228 the biomass particles, and also considering a constant density for water [38] (since its variation
229 with temperature is less than 2%) and a constant density of the holm oak wood (800 kg/m^3 , dry

230 based for holm oak species). In this sense, residence time for the liquid inside the fixed-bed
231 reactor was in the range of 1.0 min $<\tau_1<2.1$ min.

$$232 \quad \varepsilon_f = \varepsilon_0 + (1 - \varepsilon_0) \frac{(m_0 - m_f)}{m_0} \quad (1)$$

233

234 Figure 2 shows the cumulated mass of total soluble materials, oligomers and monomers of C5
235 and C6, as well as products deriving from the further reaction of sugars. These values were
236 determined using TOC and HPLC analysis of the products. The different conditions were
237 obtained by changing water flow-rates in the fractionation line for the experiments 1, 2 and 3.
238 ~~The break points shown in the curves and~~ dashed lines signals ~~present~~ the time when transition
239 between the two temperature stages takes place. The mass of soluble compounds detected by
240 TOC was calculated by dividing the value of total organic carbon concentration recognized by
241 the equipment by a factor 0.42 (Eq. (2)).

$$242 \quad r = \sum_1^c r(i) = \sum_1^c \left(\frac{m(i)}{\sum_1^c m(i)} \right) \left(\frac{n(i)MwC}{Mw(i)} \right) = 0.42; \quad i = 1..c \quad (2)$$

243 The factor r is the sum of the ratio between the molecular weight of carbon atoms in the soluble
244 compounds extracted from raw material to the molecular weight of the compounds itself. This
245 value is an approximation that allows comparing the mass obtained by TOC analysis (total
246 amount of C) with the mass quantified by HPLC (total amount of soluble compounds).

247 This approximation is based only on the sugar contents and it is used as a general value for all
248 the experiments. It does not consider the effect in the carbon ratio of the condensation and
249 dehydration reactions happening during the extraction and hydrolysis. In addition, it does not
250 take into account the amount of soluble lignin since it is relatively low (only a 4% in the raw
251 material, see section 2.2). However, in all the experiments, the mass balance matched with a
252 maximum error around 20%.

253 The overall material balance was calculated by summing the mass of the solid recovered from
254 the reactor R.1 at the end of the experiment to the mass of the soluble material estimated using
255 the quantified amount by TOC and the assumed factor showed in equation 2; and the mass of

256 insoluble lignin flushed by the water stream. For experiments 1, 2 and 3, this mass balance was
257 equal to 103.8, 93.7 and 84.9% related to the amount of biomass fed to the reactor.

258 The mass of soluble material obtained by TOC with the same values obtained by HPLC for each
259 sample are compared in the first row of graphs in Figure 2 (a). The values plotted in Figure 2
260 are the yields of soluble compounds obtained from each technique related to the same amount in
261 the raw biomass (calculated as observed soluble compounds [g]/4.65 g). The discrepancy
262 between both values is reduced when the water flow-rate through the extraction reactor is
263 increased from 11 to 26 cm³/min (23.6, -4.1 and -3.2% for the three flows, respectively). This
264 fact could be explained by the increasing production of compounds derived from the sugars
265 hydrolysis (mainly organic acids) not identified by HPLC or whose value is so low that it
266 cannot be detected. From HPLC chromatographs of experiment 1, some peaks do not fit with
267 the retention time of the 17 standard compounds identified in this column (e.g. Figure S2 in
268 Supplementary Material). Besides, some other peaks were not completely resolved. The amount
269 of sugars and soluble oligomers of C5 and C6 obtained from fractionation are displayed in the
270 second line of graphics in Figure 2 (a). Most of the hemicellulose is hydrolyzed to oligomers, in
271 fact hemicellulose is highly soluble in water because of the abundance of acetyl groups in its
272 amorphous structure [39], and after the first breaking leads to the production of soluble
273 oligomers.

274 The yield of C5 at the end of second stage of temperature was 87.3, 89.8 and 93.1%, for
275 experiments 1, 2 and 3, respectively. On the contrary, the crystalline nature confers to cellulose
276 a water insoluble character, so, the oligomers with only very low molecular weight would be
277 water soluble [40]. In this sense, when the flow rate increases in R.1 (decreasing τ_1), cellulose is
278 hydrolyzed mainly to hexoses in oligomer form, giving rise to lower amounts of monomers.
279 This result is observed by comparing the amounts of C6 oligomers (Oligo C6) to monomers
280 (C6) in experiment 1 respect to experiments 2 and 3. This selectivity to oligomers occurs mostly
281 during the first stage of temperature in R.1 (see second row of graphs in Figure 2 a). The
282 oligomers quantification was obtained from the difference between glucose, cellobiose, fructose
283 and xylose of the liquid containing all the soluble sugars and the same compounds obtained

284 from the total acid hydrolysis of this liquid [38]. So, high liquid spatial times enhanced the
285 hydrolysis and solubilization of hexoses. This distribution could be related to the difference in
286 the activation energy of the cleavage of the hydrogen bonds between celluloses and the α 1-4
287 glycosidic bond hydrolysis, which is known that is favored at subcritical conditions [10, 32].
288 The last row of graphs in Figure 2 (a) displays different amounts of products from the
289 hydrolysis of xylose, glucose and fructose. These amounts are depreciable at the first stage and
290 are increased after temperature is raised. However, these compounds are one order of magnitude
291 lower than the soluble sugars during the extraction. An example is 5-HMF, which is produced
292 mainly in the second stage of fractionation temperature where the conditions make the water a
293 highly ionic medium in the reactor R.1. The main components in the output stream were
294 pyruvaldehyde, glycolaldehyde and lactic acid. The decrease of the reaction time of liquid
295 inside the reactor diminished the further transformation of sugars.

296 *3.2 Biomass valorization with sub and supercritical water hydrolysis*

297 The outlet stream from the fixed bed reactor was fed to the SHR together with a water stream at
298 temperatures and pressures above to its critical point. The aim was to obtain a fast and selective
299 hydrolysis of the oligomers and sugars extracted from the biomass. The reaction time in the
300 supercritical reactor (t) was varied in order to modify the selectivity to different chemicals.

301 The optimum temperatures and flow-rates in R.1 have been identified in extraction step, as they
302 lead to the maximum yield of soluble material. For this reason, a flow rate of 11 cm³/s and
303 temperatures of 180° and 260°C (for the two stages, respectively) were chosen for most of the
304 experiments. Only the experiments 10 and 11 were performed with the same liquid flow-rates
305 used in the fractionation experiments 2 and 3 (17 and 26 cm³/s, respectively).

306 This approach also allows knowing the composition of the stream entering in the second reactor.
307 Eight experiments were performed, as shown in Table 1. Three temperatures and 6 reaction
308 times were tested, keeping constant the temperatures of water through the first reactor.

309 Three reactions (5, 7 and 8) were performed in a longer reactor (100 cm), aiming to increase the
310 residence time in SRH (t). A lower pressure was used in reaction 6 (162 bar) to observe the
311 influence of water density in the products distribution.

312 Overall mass balance for each experiment, calculated as described in section 3.1, is presented
313 Table 1. Mass balances indicate that no significant gasification takes place in the supercritical
314 reactor. First row of graphs in Figure 2 (b), (c) and (d) presents the mass of the soluble materials
315 quantified in the outlet stream of SHR by TOC and HPLC. The percentage yield of each
316 experiment respect to the soluble mass in the raw holm oak is presented as the number in the
317 each graph. Some differences between these two procedures are observable, mainly increasing t_e
318 in the second stage of fractionation or at higher sugars conversion. These findings could be
319 related to the production of small organic acids, ketones and aldehydes (levulinic and acrylic
320 acids, dihydroxyacetone, formaldehyde) and other compounds not identified by HPLC, see
321 Figure S2 in Supplementary Material. This hypothesis agree with the decrease of the mass
322 difference observed by both techniques when a high water flow is involved (as commented in
323 section 3.1), indicating an over breaking and oxidation of the products of interest at higher t .

324

325 *3.2.1 Oligomers and sugars conversion*

326 Oligomer conversion to C5 and C6 monomers was calculated by difference between the stream
327 entering to the SHR (composition obtained in experiment 1 corresponding to reactions 4 to 9
328 and composition of experiment 2 and 3 for experiments 10 and 11, respectively), and the stream
329 leaving the reactor after the hydrolysis.

330 The conversion of oligomers to C5 and C6 monomers are reported in the seventh column of
331 Table 1. In all the runs, oligomers conversion was higher than 85%. The exception was
332 experiment 11, in which the small t and high dilution (four times lower than in the experiments
333 4 to 8) could be the cause of the low conversion. C5 Sugars (xylose) and C6 (cellobiose, glucose
334 and fructose) are intermediate compounds in the reaction pathway. Conversion of sugars is
335 faster than cleavage of oligomers to monomers at subcritical temperatures and even at a
336 temperature a little higher than the critical point of water (e.g. 380°C). This is showed by
337 comparing the amount of Oligo C6 and Oligo C5 with C6 and C5 in experiments 4 and 6 (see
338 Figure 2 (b) and (c)). A different behavior is detected near to 400°C, like in experiment 9, where
339 oligomers conversion seems to be faster than sugars hydrolysis, in agreement with the

340 observations reported in the literature for oligomers originating from microcrystalline cellulose
341 [5][11]. Surprisingly the time needed for a complete conversion of sugars is quite larger than
342 the pure cellulose hydrolysis at the same temperature (eg. 350°C: 2 s in ref. [29] vs 12 s in this
343 work). This could be related to the hydrolysis of C5 and C6 contained inside the porous
344 structure of fluidized microparticles of biomass coming from the reactor R.1 with the stream of
345 fluidized biomass. Also the presence of other ions or compounds could be linked to this
346 attenuation.

347 *3.2.2 Added value products (AVP) from the sugars hydrolysis*

348 The third row of graphs in Figure 2 (b), (c) and (d) displays the amount of added value
349 chemicals (AVP) (glyceraldehyde, glycolaldehyde, pyruvaldehyde, lactic acid, formic acid,
350 acetic acid and 5-HMF) produced from hydrolysis of cellobiose, glucose, fructose and xylose.
351 The reaction pathway of cellulose hydrolysis involving oligomers and cellobiose as
352 intermediaries was reported in the literature [32]. Xylose hydrolysis in near critical and
353 supercritical water was analyzed by several authors [41, 42]. The combined pathway is
354 presented in Figure 3. Not all the products involved in this scheme were identified by the liquid
355 chromatography. ~~The cellulose pathway shown in Fig. 3 involves two consecutive hydrolysis,~~
356 ~~the first one in which the oligosaccharides are hydrolyzed to glucose and xylose and the second~~
357 ~~one in which glucose and xylose are involved in two possible pathways: isomerization and~~
358 ~~dehydration or retro-aldol condensation [18, 42].~~ The cellulose and hemicellulose pathways are
359 similar. They involve two consecutive hydrolysis steps, the first one in which the
360 oligosaccharides are hydrolyzed to glucose and xylose, respectively, and the second one in
361 which glucose and xylose are implicated in two possible routes: isomerization and dehydration
362 or retro-aldol condensation [18, 42]. Glucose can follow a reversible isomerization to produce
363 fructose, however, the reverse reaction is almost inhibited at the same conditions [19, 20].
364 Glucose can also be transformed into 1,6 anhydroglucose and fructose can be transformed into
365 5-hydroxymethylfurfural through a dehydration reaction [43]. The other alternative of glucose
366 conversion is the retro-aldol condensation producing glycolaldehyde and erythrose [32, 44].
367 Erythrose is further transformed into glycolaldehyde by the same reaction mechanism [18]. The

368 retro-aldol condensation reaction of fructose produces glyceraldehyde and dihydroxyacetone.
369 These molecules are further isomerized into pyruvaldehyde [19], which is transformed to lactic
370 acid by an extra oxidation. Hemicellulose hydrolysis is quite similar; the first step is the
371 depolymerization to produce xylose and xylose oligomers. After that, xylose can be isomerized
372 to D-xylulose, assuming that D-xylulose as an intermediate for furfural and retro-aldol products
373 (glyceraldehyde, pyruvaldehyde, glycolaldehyde, lactic acid, dihydroxyacetone, formaldehyde)
374 [41, 42]. This reaction pathway consists of a retro-aldol reaction (Lobry de Bruyn-Alberta van
375 Ekenstein (LBET)) from D-xylose and D-xylulose, similar to that involving D-glucose and
376 fructose.

377 In the experiments, a considerable amount of glycolaldehyde-pyruvaldehyde and lactic acid was
378 observed. The distribution of these chemicals was similar for experiments 4 and 6 (Figure 2 (b)
379 and (c)) in spite of the difference of water properties at both temperatures. At 352°C and 241.3
380 bars, the water density and pK_w are 614.7 kg/m³ and 11.7, respectively. On the other hand, at
381 383°C and 245.7 bar, those properties take a value of 319.7 kg/m³ and 15.3, both calculated as
382 developed in literature [1]. A little difference in the amount of glycolaldehyde-pyruvaldehyde as
383 well as in the 5-HMF is perceived, principally at times corresponding to the first stage of
384 temperature of the reactor R.1. This means that this variations of density and K_w , do not
385 modified largely the selectivity between isomerization-dehydration and retro-aldol pathways
386 like it does in the pure cellulose hydrolysis. In this last, isomerization of glucose to fructose is
387 highly inhibited by decreasing density [32]. This behavior could be explained by the presence of
388 of H⁺ ions coming from the acetylation taking place during the fractionation, in addition to the
389 H⁺ produced by the water ionization. Also, considering the nature of raw biomass, other ions in
390 solution could be present. Under 352 °C and pressure, isomerization of glucose to fructose and
391 further dehydration is favored for pure cellulose hydrolysis [43]. But, in the present cases, the
392 high yields of glycolaldehyde-pyruvaldehyde and lactic acid are evidences that the retro-aldol
393 pathways take place as well. Experiments 4 and 5 were performed at similar temperature and
394 pressure but involving different residence times ($t=1.06$ vs 11.15 s, respectively). For
395 experiment 5, the acetic acid amount was highly increased, mostly in the time period

396 corresponding to the first stage of temperature in R.1. This acetic acid exceeded the amount
397 produced in the hemicellulose deacetylation. ~~The retro-aldol pathway coming from xylose by~~
398 ~~means of glyceraldehyde route, could explain the difference of acetic acid obtained directly~~
399 ~~from lactic acid decarboxylation. This extra amount of acetic acid could not be considered only~~
400 ~~from the hemicellulose source, since there is also a large concentration of C6 in the first fraction~~
401 ~~of the feed stream (see Figure 2 (a)). This C6 portion could also contribute to the~~
402 ~~glyceraldehyde route.~~ Besides, acetic acid could be obtained directly from lactic acid
403 decarboxylation [15]. Both, glucose and xylose, are able to produce lactic acid by means of the
404 retro-aldol pathway with glyceraldehyde and pyruvaldehyde as intermediaries (see Figure 3). In
405 this sense, these retro-aldol pathways could explain the extra amount of acetic acid obtained at
406 longer residence times in the SHR. Figure 4, displays the pH of the output stream after the
407 fractionation stage (experiment 1) and the coupled process fractionation+hydrolysis
408 (experiments 4, 5, 6 and 8). The pH in the outlet stream, after SHR, was always lower to the pH
409 of the output stream from the fractionation step itself. ~~comparing the H⁺ concentration of the~~
410 ~~experiments during the time period of the first stage during the extraction.~~ This observation
411 agrees with the fact that extra amount of acetic acid was produced when a deeper hydrolysis was
412 performed (see experiments 5 and 8). After this ~~time period~~, no difference in the pH can be
413 detected. Similar behavior was observed from experiments 6 and 8, ~~however, in this case, larger~~
414 ~~amount of formic acid was observed compared to the experiments above mentioned~~ in spite of
415 the difference of formic acid produced in both (see Figure 2 (c)).

416 The pressure change in the range studied, had no effect on the chemicals distribution (see Figure
417 2 (c), experiments 6 and 7). Under the conditions of experiment 7, pK_w is 11.9, calculated by
418 means of an empiric equation [45]. This value is quite similar than pK_w of the experiment 6. In
419 this way, in spite of density change, the same AVP distribution is observed. Longer residence
420 time of experiment 7 explains the difference in oligomers with experiment 6. The distribution of
421 the AVP of experiment 6, is independent of the change in pK_w, as was discussed above for
422 experiments 4 and 6. The highest yield of glycolaldehyde-pyruvaldehyde (calculated as mass of

423 product/mass of soluble material in raw biomass) was obtained for experiment 7 (24.4%),
424 probably due to the combination of higher H⁺ concentration and longer *t*.

425 A different AVP distribution is observed in the experiment 9, where lactic acid is the most
426 abundant product and acetic acid is depleted compared to the experiment 4 and 6 (see Figure 2
427 (d)). This finding could be explained by the short *t* of the mixture at high temperature,
428 conditions in which the reactions are stopped ~~before~~ after lactic acid production in the retro-
429 aldol route, inhibiting the acetic acid formation. This selectivity seems to take place in the SHR
430 mainly during the first stage of temperature in the reactor R.1. After that, the formation of lactic
431 acid in the SHR is reduced. ~~This selectivity seems to take place mainly during the time period of~~
432 ~~the first stage of the fractionation, because after that, the formation of lactic acid as well as of~~
433 ~~glycolaldehyde-pyruvaldehyde is lower.~~ The highest yield of lactic acid was found at
434 Experiment 9 (25.5%). The water flow increase in the first reactor has no clear effect on the
435 production of retro-aldol compounds (see reactions 10 and 11 in Figure 2 (d)). Under these
436 conditions, the oligomers breakup seems to become slower, since their amount is enlarged
437 related to the monomeric sugars. In both cases, the retro aldol pathways are followed producing
438 glycolaldehyde-pyruvaldehyde and lactic acid with similar yields.

439 The combination of many variables influencing the distribution of a large number of
440 products, involved in a complex reaction path as the described in Fig. 3, is hard to be easily
441 explained. Furthermore, as was mentioned above, we are dealing with the hydrolysis of a real
442 biomass, in which other components could be influencing the observed behavior.

443 **3.3 Hydrolysis kinetic model**

444 Aiming to analyze further the results obtained by the coupled system, a kinetic model for the
445 second reactor is proposed in this section. This model takes into account the solubilized biomass
446 composition fed to the second reactor. It was specially focused on the time period corresponding
447 to the first stage of the solubilization (at the conditions of experiment 1) since this step produces
448 an outlet stream with higher amount of the chemicals of interest (see last two columns of Table
449 1). The bigger added valued compounds production from stage 1 is due to the fact that the
450 operational temperature was around 180 °C, which means a lower degradation. The reaction

451 pathway proposed in this case, showed in Figure 45. It is a simplified version of the real
 452 hydrolysis described in Figure 3. The modelling was done by the transient regime mass balances
 453 for each compound in the fluid: oligomers, sugars and products (Eq. (3)). Moreover, the
 454 following assumptions have been considered: (1) the reaction order for all the kinetics is 1 for
 455 the biomass compound and proton concentration in water, (2) there are no diffusional effects in
 456 fluid phase, (3) kinetic constants follows Arrhenius' law and (4) the reactor works at the same
 457 temperature at any point. Regarding kinetics, a conventional expression was used including the
 458 effect of the concentration of water proton since it is a hydrolysis process (Eq. (4)).

$$\frac{\delta C_{Lj}}{\delta t} = r_j - \frac{u}{L} \cdot \frac{\delta C_{Lj}}{\delta z} \quad (3)$$

$$r_j = C_{H^+} \cdot \sum_{i=1}^{i=N} \alpha_{i,j} \cdot K_{Li} \cdot C_{Li} \quad (4)$$

459

460 3.3.1 Numerical resolution

461 Eq. (3) is a set of 6 partial differential equations (PDE) which has to be discretized to obtain a
 462 set of ordinary differential equation (ODE). The resolution of this set of ODEs was performed
 463 by the Runge-Kutta's method with a 8th convergence order and the discretization by coupling
 464 orthogonal collocation method on finite elements [46]. The fitting of the experimental data
 465 constitutes an optimization problem. Due to its complexity, it was previously seeded by manual
 466 iteration, and then, optimized by the Nelder-Mead-Simplex method. Moreover, as the inlet
 467 concentration of the hydrolysis reactor was variable and the oligomer properties changed with
 468 extraction time [47], the problem was optimized at every experimental point. Finally, the
 469 solution was reviewed in order to ensure the physical meaning of the parameters. The objective
 470 function was the minimization of the Absolute Average Deviation (A.A.D., Eq. (5)) for
 471 oligomer, sugar and products concentration at the SHR output.

472

$$A. A. D. = \sum_{i=1}^n \frac{1}{n} \cdot \left| \frac{X_{exp} - X_{sim}}{X_{exp}} \right| \cdot 100 \quad (5)$$

473

474

475 3.3.2 Experimental data fittings

476 In order to validate the model, only experiments 4, 6 and 9 were used because they were
477 carried out at similar residence times and three different temperatures (see Table 1). For
478 experiment 4, the data at extraction time of 9 and 14 min were not considered because they do
479 not follow the tendency fixed by the set of the three experiments used (4, 6 and 9). Moreover, as
480 each experiment was carried out independently, the inlet for the reactor was assumed to have the
481 same composition that experiment 3 but with TOC profile of the fitted experiment (4, 6 and
482 9). It is also remarkable that the volumetric flow was the addition of the provided flow by the
483 two pumps for all the experiments (see Figure 1). The deviation between the model and the
484 experimental data is arrayed in Table 2 and for experiment 6 it also can be seen in Figure 6. The
485 model was able to reproduce successfully the hydrolysis of solubilized biomass, being the
486 average A.A.D. 21.14 %, 37.37 %, 18.41 % and 7.24 % for instant hemicellulose and cellulose
487 oligomers, sugars C6, sugars C5 and their degradation products (the added value products
488 respectively or AVP). These discrepancies changed to 27.46 %, 7.61 %, 9.31 % and 3.99%
489 respectively when cumulated values were used. Taking into account these last values, it can be
490 checked that the highest error is in the estimation of the oligomers mass, which can be caused
491 by the fact that the experimental data were obtained by the difference between the TOC and the
492 sum of the other compounds (sugars and AVP). Moreover, the deviation between the
493 experimental and simulated TOC was also calculated in order to check that the mass
494 conservation law is followed. For all the cases, this mass balance deviation result in zero percent
495 with three significant figures (0.00%). The kinetic constants and the stoichiometric coefficients
496 (K_{L_i} and $\alpha_{i,j}$ in Eq. (4), respectively) had to be obtained from fitting. Regarding to $\alpha_{i,j}$, it was
497 always 1 less for the final products coming from hemicellulose oligomers since they are
498 composed by pentoses and hexoses [48, 49]. These fitted parameters, which are shown in Table
499 4, require a deeper analysis and they are discussed in the next section.

500 3.3.3 Analysis of kinetic parameters

501 The dependence of the kinetics parameters with temperature was proved. The regression
502 coefficient (R^2) according the Arrhenius' theory was higher than 0.84 for all the cases (see

503 Table 3). No change in the kinetic behavior was observed through the critical point (see Table
 504 3) like does in the hydrolysis of microcrystalline cellulose [44, 50] according to the commented
 505 in section 3.2.2, since there is not simultaneous solubilization in the SHR. However, a
 506 dependence of the kinetic behavior was observed with the extraction time, since the rates of
 507 production of valuable chemicals is decreased after the maximum of solubilized mass is reached
 508 (see Figure 7 (a) and (b)). This observation could be related with the influence of some of the
 509 chemicals produced by the further hydrolysis of sugars on the hydrothermal hydrolysis. In
 510 addition, it is also interesting that after this change, the kinetics of the sugar transformation tend
 511 to their initial value while the kinetic of the oligomer breakdown grows exponentially. This
 512 difference would be originated by the changes in the molecular weight of the extracted
 513 oligomers and the fact that they would be transformed more quickly if the molecular weight is
 514 lower. Moreover, it can be seen that temperature can compensate this negative effect, being
 515 negligible for oligomers at 400°C (Figure 7 (c)).

516 Other interesting result is the evolution of the ratio between the four kinetic constants. In
 517 section 3.2.1 it was indicated that sugar transformation is faster than oligomer cleavage in
 518 subcritical conditions and lower in supercritical water. This behavior agrees with the obtained
 519 from the fittings, but only before the time of maximum of extraction (Figure 7 (a) and (c)). So,
 520 from this point, the changes in molecular weight and the raw material transformation makes the
 521 oligomer cleavage always greater. As the oligomer composition changes with extraction time,
 522 the kinetic cannot be reproduced by a typical Arrhenius' kinetic. So, two equations function of
 523 this time (t_e) are proposed, one for the ~~pre-exponential factor~~ oligomer cleaving (Eq. 46) and
 524 other for the ~~activation energy~~ sugar further reactions (Eq. 57).

$$525 \quad P = C \cdot |t_{e_{\max}} - A \cdot t_e|^B \quad (46)$$

526

$$527 \quad P = D + \frac{E}{1 + e^{(F \cdot (t_e - G))}} \quad (57)$$

528

529 Where P refers to both, the activation energy (E_a/R) and the natural logarithm of the pre-
530 exponential factor ($\ln(k)$). In Eq. 46, the parameter C is the natural logarithm of the pre
531 exponential factor or activation energy at the maximum extraction time ($t_{e_{max}}$) and parameters
532 A and B introduce the effect of the changes in the structure and reaction medium. A would be
533 related with the strength of the compound against its degradation by hydrolysis. B would be a
534 measure of how structure or reaction medium can accelerate or restrain the degradation. In Eq.
535 57, D is the pre exponential factor or the activation energy at the time where the biggest
536 solubilization takes place, E and F , are the parameters that consider the role of the structure and
537 reaction medium and G is the time when the maximum extraction is reached. In this case, E
538 would represent how the medium or the structure can enhance the hydrolysis or hinder it. F
539 would be the compound resistance against degradation.

540 Finally, the evolution of the hexoses content in hemicellulose oligomers is represented in
541 Figure 7 (b). It can be observed that the ratio between these values grows with time. This result
542 was expected because hexoses would make the dissolution more difficult and would explain the
543 fact that in experiment 5 the extraction was faster than 4 and 9 experiments (see Figure 7 (c)).
544 Moreover this result agrees with the data reported by other authors [51].

545 3.3.4 Simulated experiments

546 As it was mentioned in section 3.3.2, only experiments 4, 6 and 9 were used to validate the
547 model. Experiments 5 and 8 were not considered because their reaction time were much higher,
548 which implies almost a total conversion at the reactor outlet. However, it checked if the model
549 was able to reproduce their behavior. The result of the simulations are presented in Figure 8,
550 being the absolute deviation around 4% for both experiments. Therefore, the model can predict
551 successfully the hydrolysis at both low (0.2 – 1.0 s) and high (11.1-12.5 s) residence times.

552 3.3.5 Model limitations

553 From the results showed in the three previous sections, the model was able to successfully
554 reproduce the experimental behavior of the set-up. In fact, this model can be used for any other
555 lignocellulosic biomass because of the fact that it has been developed for a general biomass
556 hydrolysis pathway. However, it is limited to processes where soluble lignin is low and when

557 the aim is to reproduce the overall behavior of a solubilized biomass stream hydrolysis instead
558 of an analysis of each individual compound. Furthermore, this model can be also adapted to
559 processes where the inlet stream is variable in time.

560 **Conclusions**

561 A new process coupling fractionation and hydrolysis steps was developed. By means of this
562 process, up to 64.2% of feed Holm oak wood was solubilized mainly as oligomers of hexoses
563 and pentoses and sugars with a small fraction of retro-aldol compounds. The low ratio of the
564 amount of oligomers to monomeric sugars in the outlet stream could be explained by a similar
565 behavior than in the case of pure cellulose hydrolysis: the rate of monomers hydrolysis is higher
566 to the oligomers break up in subcritical conditions, but this tendency is reverted at supercritical
567 temperatures.

568 The main products of the further hydrolysis in the second reactor were glycolaldehyde,
569 pyruvaldehyde and lactic acid. Yield (related to the amount of soluble sugars in the raw
570 biomass) of 24 wt% of Glycolaldehyde-Pyruvaldehyde was found at long reaction times (350°C,
571 160bar and 8,6 s) and 25 wt% of lactic acid was found at short reaction time but high
572 temperature (400°C, 250 bar and 0.23s). An increasing amount of acetic acid was observed at
573 the highest residence times (e.g. 12 s).

574 The distribution of products is related with a combined reaction hydrolysis pathway of
575 cellulose and hemicellulose involving oligomer cleavage to monomers, isomerization steps and
576 two competing paths: Retro-aldol condensation and dehydration. The influence of the water
577 density and the amount of ions H^+ coming from the dissociation process is not clear as it is in
578 the case of the hydrolysis of pure cellulose, in which the glucose dehydration is highly inhibited
579 and retro aldol pathways clearly favored at temperatures and pressures above the water critical
580 point. In the present work, products coming from retro-aldol paths as well as products of
581 dehydration are observed in both conditions: sub and supercritical. Finally, a general kinetic
582 modelling for the hydrolysisreactor was proposed. This model could reproduce the experimental
583 data for sugar and added value products with deviations lower than 10%. Besides, the calculated
584 kinetic parameters reproduced the changes in oligomer and sugar conversion when the

585 hydrolysis is performed in supercritical conditions instead of in subcritical water. This model
586 can be applied to any other lignocellulosic biomass with a low content of soluble lignin.

587 The main advantage of this combined process consist in providing a liquefied biomass
588 stream to a selective hydrolysis reactor giving the valorization of the raw material avoiding the
589 costly grinding of particles from several millimeters to less than two hundred microns needed to
590 pump it in a water stream belonging to a high pressure process.

591

592 **Acknowledgements**

593 The authors acknowledge the Spanish “Ministerio de Economía y Competitividad
594 (MINECO)” and FEDER funds, Project BioFraHynery CTQ2015-64892-R and the regional
595 government (Junta de Castilla y León), Project Reference: VA330U13 for funding. MEng.
596 Gianluca Gallina wishes to acknowledge the Spanish “Ministerio de Economía y
597 Competitividad (MINECO)” for the scholarship/predoctoral contract BES-2013-063556. MEng.
598 Alvaro Cabeza would like to thank to the Spanish “Ministerio de Educación, Cultura y
599 Deporte”, training program of university professors (reference FPU2013/01516) for the research
600 training contract.

601

602 **Abbreviations and symbols**

603 *Acronyms*

604

605 A.A.D.: Average absolute Deviation.

606 Olig: Hemicellulose and cellulose oligomers.

607 C6/OligC5: ratio hexoses to hemicellulose oligomers.

608 *Greek letters and symbols*

609

610 A-G: Parameters for kinetics constant estimation.

611 $\alpha_{i,j}$: Stoichiometric coefficient of the compound “j” for the reaction “i”, dimensionless.

612 C_{H^+} : Concentration of the protons, mg/L.

613 C_{Lj} : Concentration of the compound “j”, mg/L. E_d/R : Activation energy, K.

614 ε : Porosity of the bed, dimensionless.

615 ε_f : Porosity of the bed, calculated at the end of the experiment, dimensionless.

616 ε_{av} : Average porosity of the bed, between the beginning and the end of the experiment,
617 dimensionless.

618 ε_o : Porosity of the bed, calculated at the end of the experiment, dimensionless.

619 K_{L_i} : Kinetic constant, min^{-1} .

620 k : Pre-exponential factor of the kinetic constant, $\text{mg}^{-1} \cdot \text{min}^{-1}$.

621 L : Length of the reactor, m. m_0 : initial mass of the solid in the reactor, g.

622 m_f : final mass of the solid in the reactor, g.

623 $m(i) (RM)$: total amount of component (i) in the raw material, extracted by acid hydrolysis and
624 detected by HPLC analysis, g.

625 $Mw(i)$: molecular weight of component i, g/mol.

626 MwC : molecular weight of the a carbon atom, g/mol.

627 $m_{sol,tot}(RM)$: total amount of soluble compounds in the raw material, extracted by acid
628 hydrolysis and detected by HPLC analysis, g.

629 N : Number of compounds, dimensionless.

630 n : Total number of experiments, dimensionless.

631 $n(i)$: Number of carbon atoms in the soluble component i , dimensionless.

632 P : Calculated kinetic parameter, activation energy or the natural logarithm of the pre-
633 exponential factor

634 R^2 : Coefficient R^2 , dimensionless.

635 r : ratio between the molecular weight of the soluble compounds extracted and the molecular
636 weight of the atoms of carbon, dimensionless.

637 $r(i)$: ratio between the molecular weight of the soluble compounds extracted and the molecular
638 weight of the atoms of carbon for compound i , dimensionless.

639 r_j : Reaction rate of the compound “j”, mg/min·L.

640 u : Liquid velocity in the reactor, m/min.

641 t : Residence time in the SHR, s.

642 t_e : Extraction time, min.

643 $t_{e_{max}}$: Maximum extraction time, min.

644 $x_{i_{EXP}}$: Experimental value of the fitted variable.

645 $x_{i_{SIM}}$: Simulated value of the fitted variable.

646 z : Coordinate along the length of the reactor, dimensionless.

647

648

649

650

651

652

- 654 [1] N. Akiya, P.E. Savage, Roles of Water for Chemical Reactions in High-Temperature Water,
655 Chemical Reviews 102 (2002) 2725-2750.
- 656 [2] P.E. Savage, S. Gopalan, T.I. Mizan, C.J. Martino, E.E. Brock, Reactions at supercritical
657 conditions: Applications and fundamentals, AIChE Journal 41 (1995) 1723–1778.
- 658 [3] D.A. Cantero, M.D. Bermejo, M.J. Cocero, Reaction engineering for process intensification
659 of supercritical water biomass refining, The Journal of Supercritical Fluids (2014)
660 doi:10.1016/j.supflu.2014.1007.1003.
- 661 [4] A.J. Ragauskas, C.K. Williams, B.H. Davison, G. Britovsek, J. Cairney, C.A. Eckert, W.J.
662 Frederick, J.P. Hallett, D.J. Leak, C.L. Liotta, J.R. Mielenz, R. Murphy, R. Templer, T.
663 Tschaplinski, The Path Forward for Biofuels and Biomaterials, Science 311 (2006) 484 -489.
- 664 [5] A.A. Peterson, F. Vogel, R.P. Lachance, M. Fröling, J.M.J. Antal, J.W. Tester,
665 Thermochemical biofuel production in hydrothermal media: A review of sub- and supercritical
666 water technologies, Energy & Environmental Science 1 (2008) 32.
- 667 [6] D.A. Cantero, C. Martinez, M.D. Bermejo, M.J. Cocero, Simultaneous and selective
668 recovery of cellulose and hemicellulose fractions from wheat bran by supercritical water
669 hydrolysis, Green Chemistry DOI: 10.1039/c4gc01359j (2015).
- 670 [7] P. Gullón, A. Romani, C. Vila, G. Garrote, J.C. Parajó, Potential of hydrothermal treatments
671 in lignocellulose biorefineries, Biofuels, Bioproducts and Biorefining 6 (2012) 219-232.
- 672 [8] T.H. Kim, Y.Y. Lee, Fractionation of corn stover by hot-water and aqueous ammonia
673 treatment, Bioresource Technology 97 (2006) 224-232.
- 674 [9] M. Sasaki, T. Adschiri, K. Arai, Fractionation of sugarcane bagasse by hydrothermal
675 treatment, Bioresource Technology 86 (2003) 301-304.
- 676 [10] M. Sasaki, T. Adschiri, K. Arai, Kinetics of cellulose conversion at 25 MPa in sub- and
677 supercritical water, AIChE Journal 50 (2004) 192-202.
- 678 [11] D.A. Cantero, M. Dolores Bermejo, M. José Cocero, High glucose selectivity in
679 pressurized water hydrolysis of cellulose using ultra-fast reactors, Bioresource Technology 135
680 (2013) 697-703.
- 681 [12] Z. Fang, C. Fang, Complete dissolution and hydrolysis of wood in hot water, AIChE
682 Journal 54 (2008) 2751-2758.
- 683 [13] H.R. Holgate, J.C. Meyer, J.W. Tester, Glucose hydrolysis and oxidation in supercritical
684 water, AIChE Journal 41 (1995) 637–648.
- 685 [14] Y. Chen, Y. Wu, R. Ding, P. Zhang, J. Liu, M. Yang, P. Zhang, Catalytic hydrothermal
686 liquefaction of *D. tertiolecta* for the production of bio-oil over different acid/base catalysts,
687 AIChE Journal 61 (2015) 1118-1128.

688 [15] Y. Wang, F. Jin, M. Sasaki, Wahyudiono, F. Wang, Z. Jing, M. Goto, Selective conversion
689 of glucose into lactic acid and acetic acid with copper oxide under hydrothermal conditions,
690 *AIChE Journal* 59 (2013) 2096–2104.

691 [16] X. Yan, F. Jin, K. Tohji, A. Kishita, H. Enomoto, Hydrothermal conversion of
692 carbohydrate biomass to lactic acid, *AIChE Journal* 56 (2010) 2727-2733.

693 [17] O. Bobleter, Hydrothermal degradation of polymers derived from plants, *Progress in*
694 *polymer science* 19 (1994) 797-841.

695 [18] M. Sasaki, K. Goto, K. Tajima, T. Adschiri, K. Arai, Rapid and selective retro-aldol
696 condensation of glucose to glycolaldehyde in supercritical water, *Green Chemistry* 4 (2002)
697 285-287.

698 [19] B.M. Kabyemela, T. Adschiri, R. Malaluan, K. Arai, Degradation Kinetics of
699 Dihydroxyacetone and Glyceraldehyde in Subcritical and Supercritical Water, *Industrial &*
700 *Engineering Chemistry Research* 36 (1997) 2025-2030.

701 [20] B.M. Kabyemela, T. Adschiri, R.M. Malaluan, K. Arai, Glucose and Fructose
702 Decomposition in Subcritical and Supercritical Water: Detailed Reaction Pathway,
703 Mechanisms, and Kinetics, *Industrial & Engineering Chemistry Research* 38 (1999) 2888-2895.

704 [21] B.M. Kabyemela, T. Adschiri, R.M. Malaluan, K. Arai, Kinetics of Glucose Epimerization
705 and Decomposition in Subcritical and Supercritical Water, *Industrial and Engineering*
706 *Chemistry Research* 36 (1997) 1552-1558.

707 [22] X. Lü, S. Saka, New insights on monosaccharides' isomerization, dehydration and
708 fragmentation in hot-compressed water, *The Journal of Supercritical Fluids* 61 (2012) 146-156.

709 [23] Y. Román-Leshkov, M. Moliner, J.A. Labinger, M.E. Davis, Mechanism of Glucose
710 Isomerization Using a Solid Lewis Acid Catalyst in Water, *Angewandte Chemie International*
711 *Edition* 49 (2010) 8954–8957.

712 [24] M. Bicker, S. Endres, L. Ott, H. Vogel, Catalytical conversion of carbohydrates in
713 subcritical water: A new chemical process for lactic acid production, *Journal of Molecular*
714 *Catalysis A: Chemical* 239 (2005) 151-157.

715 [25] M. Bicker, D. Kaiser, L. Ott, H. Vogel, Dehydration of d-fructose to
716 hydroxymethylfurfural in sub- and supercritical fluids, *The Journal of Supercritical Fluids* 36
717 (2005) 118-126.

718 [26] D.C. Elliott, P. Biller, A.B. Ross, A.J. Schmidt, S.B. Jones, Hydrothermal liquefaction of
719 biomass: Developments from batch to continuous process, *Bioresource Technology* 178 (2015)
720 147-156.

721 [27] W. Reynolds, H. Singer, S. Schug, I. Smirnova, Hydrothermal flow-through treatment of
722 wheat-straw: Detailed characterization of fixed-bed properties and axial dispersion, *Chemical*
723 *Engineering Journal* 281 (2015) 696-703.

724 [28] Y. Yu, H. Wu, Effect of ball milling on the hydrolysis of microcrystalline cellulose in hot-
725 compressed water, *AIChE Journal* 57 (2011) 793-800

726 [29] Y. Zhao, S. Zhang, J. Chen, Mechanisms of sequential dissolution and hydrolysis for
727 lignocellulosic waste using a multilevel hydrothermal process, *Chemical Engineering Journal*
728 273 (2015) 37-45.

729 [30] M.J. González-Muñoz, S. Rivas, V. Santos, J.C. Parajó, Aqueous processing of Pinus
730 pinaster wood: Kinetics of polysaccharide breakdown, *Chemical Engineering Journal* 231
731 (2013) 380-387.

732 [31] S. Kilambi, K.L. Kadam, Production of fermentable sugars and lignin from biomass using
733 supercritical fluids, US Patent, Google Patents, United States of America, 2013.

734 [32] D.A. Cantero, M.D. Bermejo, M.J. Cocero, Kinetic analysis of cellulose depolymerization
735 reactions in near critical water, *Journal of Supercritical Fluids* 75 (2013) 48-57.

736 [33] A.H. Sluiter, B; Ruiz, R; Scarlata, C; Sluiter, J; Templeton, D; Crocker D, Determination
737 of Structural Carbohydrates and Lignin in Biomass, National Renewable Energy Laboratory,
738 U.S. Department of Energy, Golden, Colorado, 2011.

739 [34] A.H. Sluiter, B; Ruiz, R; Scarlata, C; Sluiter, J; Templeton D, Determination of Sugars,
740 Byproducts, and Degradation Products in Liquid Fraction Process Samples, National Renewable
741 Energy Laboratory, U.S. Department of Energy, Golden, Colorado, 2006.

742 [35] P. Mäki-Arvela, T. Salmi, B. Holmbom, S. Willför, D.Y. Murzin, Synthesis of Sugars by
743 Hydrolysis of Hemicelluloses- A Review, *Chemical Reviews* 111 (2011) 5638-5666.

744 [36] X.-F.C. S.-N. Sun, H.-Y. Li, F. Xu, R.-C. Sun, Structural characterization of residual
745 hemicelluloses from hydrothermal pretreated Eucalyptus fiber., *International Journal of*
746 *Biological Macromolecules* 69 (2014) 158-164.

747 [37] R. Fletcher, A Modified Marquardt Subroutine for Nonlinear Least Squares, United
748 Kingdom Atomic Energy Authority, Harwell, 1971.

749 [38] G. Gallina, Á. Cabeza, P. Biasi, J. García-Serna, Optimal conditions for hemicelluloses
750 extraction from Eucalyptus globulus wood: hydrothermal treatment in a semi-continuous
751 reactor, *Fuel Processing Technology* 148 (2016) 350-360.

752 [39] B.A. Miller-Chou, Koenig, J.L., A review of polymer dissolution, *Progress in Polymer*
753 *Science* 28 (2003) 1223-1270.

754 [40] Y. Zhao, W.J. Lu, H.T. Wang, Supercritical hydrolysis of cellulose for oligosaccharide
755 production in combined technology, *Chemical Engineering Journal* 150 (2009) 411-417.

756 [41] Sasaki M., Hayakawa T., Arai K., Adschiri T., Measurement of the Rate of Retro-Aldol
757 Condensation of d-Xylose in Subcritical and Supercritical Water., in: W.S.P. Co. (Ed.) 7th
758 International Symposium Hydrothermal ReactionsSingapore, 2003, pp. 169-176.

759 [42] Aida T.M., Shiraishi N., Kubo M., Watanabe M., Smith Jr. RL, Reaction kinetics of d-
760 xylose in sub- and supercritical water, *Journal of Supercritical Fluids* 55 (2010) 208-216.

761 [43] H. Kimura, M. Nakahara, N. Matubayasi, In Situ Kinetic Study on Hydrothermal
762 Transformation of d-Glucose into 5-Hydroxymethylfurfural through d-Fructose with ¹³C NMR,
763 The Journal of Physical Chemistry A 115 (2011) 14013-14021.

764 [44] D.A. Cantero, Á. Sánchez Tapia, M.D. Bermejo, M.J. Cocero, Pressure and temperature
765 effect on cellulose hydrolysis in pressurized water, Chemical Engineering Journal 276 (2015)
766 145-154.

767 [45] W.L. Marshall, E.U. Franck, Ion product of water substance, 0–1000 °C, 1–10,000 bars
768 New International Formulation and its background, Journal of Physical and Chemical Reference
769 Data 10 (1981) 295-304.

770 [46] W. Press, S. Teukolsky, W. Vetterling, B. Flannery, Numerical recipes 3rd edition: The art
771 of scientific computing, (2007).

772 [47] A. Cabeza, C.M. Piqueras, F. Sobrón, J. García-Serna, Modeling of biomass fractionation
773 in a lab-scale biorefinery: Solubilization of hemicellulose and cellulose from holm oak wood
774 using subcritical water, Bioresource Technology 200 (2016) 90-102.

775 [48] O. Bobleter, Hydrothermal degradation of polymers derived from plants, Progress in
776 Polymer Science (Oxford) 19 (1994) 797-841.

777 [49] W.H. P. Harmsen, L. Bermudez, R. bakker, Literature review of physical and chemical
778 pretreatment processes for lignocellulosic biomass, Wageningen UR Food & Biobased
779 Research, 2010.

780 [50] M. Sasaki, B. Kabyemela, R. Malaluan, S. Hirose, N. Takeda, T. Adschiri, K. Arai,
781 Cellulose hydrolysis in subcritical and supercritical water, The Journal of Supercritical Fluids
782 13 (1998) 261-268 %U <http://www.sciencedirect.com/science/article/pii/S0896844698000606>.

783 [51] S.-N. Sun, X.-F. Cao, H.-Y. Li, F. Xu, R.-C. Sun, Structural characterization of residual
784 hemicelluloses from hydrothermal pretreated Eucalyptus fiber, International journal of
785 biological macromolecules 69 (2014) 158-164.

786

787

788 **List of Tables**

789 **Table 1.** Temperatures, pressures, residence times, mass balance and oligomers conversions of
790 the experiments coupling Fractionation+Hydrolysis reactors.

791 ^a Residence times were calculated based on the concepts drawn in reference [32].

792 ^b Mass balance accounts the amount of solid recovered from the Extraction reactor adding the
793 mass of insoluble lignin flushed in the water stream and the total mass solubilized measured by
794 TOC.

795 ^c Oligomers conversion involves the mass of oligomers quantified by HPLC outcoming from the
796 Fractionation related to the mass of oligomers in the outlet stream of the sub-supercritical
797 reactor.

798 **Table 2.** Average absolute deviation of the fittings (experiments 4, 6 and 9) and simulations
799 (experiments 5 and 8).

800 **Table 3.** Regression coefficient (R^2) of the Activation Energy with temperature for the kinetic
801 constants showed in Figure 5.

802 **Table 4.** Fitted parameters used to estimate the kinetic constants depending on the extraction
803 time.

804 **List of Figures**

805 **Figure 1.** Experimental setup coupling fractionation and hydrolysis reactors.

806 D.1, D.2: Deionized water deposits. P.1: American Lewa EK6 2KN High pressure piston pump.
807 P.2: Milton Roy XT membrane pump. V.1, V.2: Parker check valve. H.1: Electric low
808 temperature heater, 100 cm of 1/8 in SS316 piping and 2 kW resistor. H.2: 1800 cm of 1/8 in
809 SS316 piping and, high temperature heater and 10 kW resistor. R.1: Fractionation reactor, 40
810 cm length, 1/2 in O.D. SS316 piping. V.2: Parker relief valve. R.2: Second Reactor (SHR) built
811 with 1/4 in O.D. SS316 tubing. Two reactors sizes were used 11 cm and 100 cm of length. V.3:
812 Parker relief valve. V.4: high temperature valve Autoclave Engineers 30VRMM4812. IE: 200
813 cm of concentric tube heat exchanger 1/2 in- 1/4 in. V5: Three way Parker valve. D.3: Falcon®
814 flasks. D.4: 25 L polyethylene products deposit.

815

816

817 **Figure 2.** Product distribution and mass balance in the biomass valorization.

818 (a) Results from the fractionation without further hydrolysis for 11, 17 and 26 cm³/min in
819 the extraction line. The first line of graphs represents to the percentage of soluble
820 compounds identified by total organic carbon (TOC) and HPLC. The yields, calculated
821 by the obtained soluble fractions [g] / (4.65 g), are showed above each curve. Second
822 row of graphs in Figure 2 shows the amount of carbohydrates in the form of sugars and
823 oligomers. The last row displays the time evolution of the products derived from the
824 hydrolysis of sugars in the fixed bed reactor.

825 (b) Products distribution at 380°C

826 (c) Product distribution at 350°C

827 (d) Product distribution at 400°C and short residence times.

828 In experiment 11, the absence of water flux in Reactor 1 makes heating process it faster
829 (5 min). We choose this option in order to avoid a large transition state.

830 **Figure 3.** Combined reaction pathway of oligomers C5 and C6 including the glucose and xylose
831 further reactions in hot pressurized water.

832 **Figure 4.** pH of the liquid product vs time. Comparison of the reactions at low (experiments 4
833 and 6) and high conversions (experiments 5 and 8) at sub and supercritical conditions of water.

834 **Figure 5.** Simplified reaction pathway for solved biomass hydrolysis.

835 **Figure 6.** Experimental and simulated amounts of soluble material by TOC, C5+C6 Oligomers,
836 sugars C6, sugars C5 and added value products obtained in experiment 6.

837 Symbols represents the experimental values and continuous lines represents the results of the
838 kinetic model using the optimized kinetic parameters.

839 **Figure 7.** Evolution of the logarithm of the kinetic constants for experiment 6(a), 4(b) and 9 (c).

840 Ratio C6/OligoC5 (d). Solubilized mass with the extraction time for the experiments 6, 4 and 9

841 (e).

842 k_1 : Cellulose oligomer breakup kinetic constant, k_2 : Hemicellulose oligomer breakup kinetic
843 constant, k_3 : Sugars C6 hydrolysis kinetic constant, k_4 : Sugars C5 hydrolysis kinetic.

844 **Figure 8.** Comparison between the experimental and simulated data for AVP in experiment 5
845 and 8.

846 Symbols are the experimental data and full lines shows the prediction of the model with
847 optimized kinetic parameters for each data.

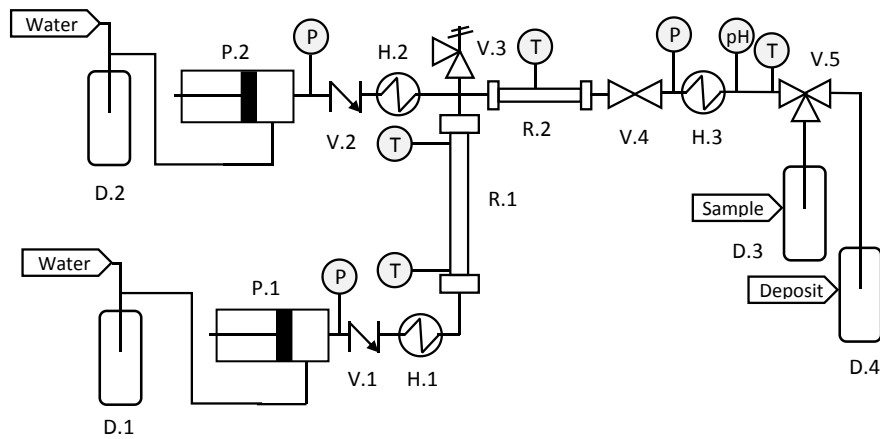
848

849

Figure 1.

850

851



858

859

860

861

862

863

864

865

866

867

868

869

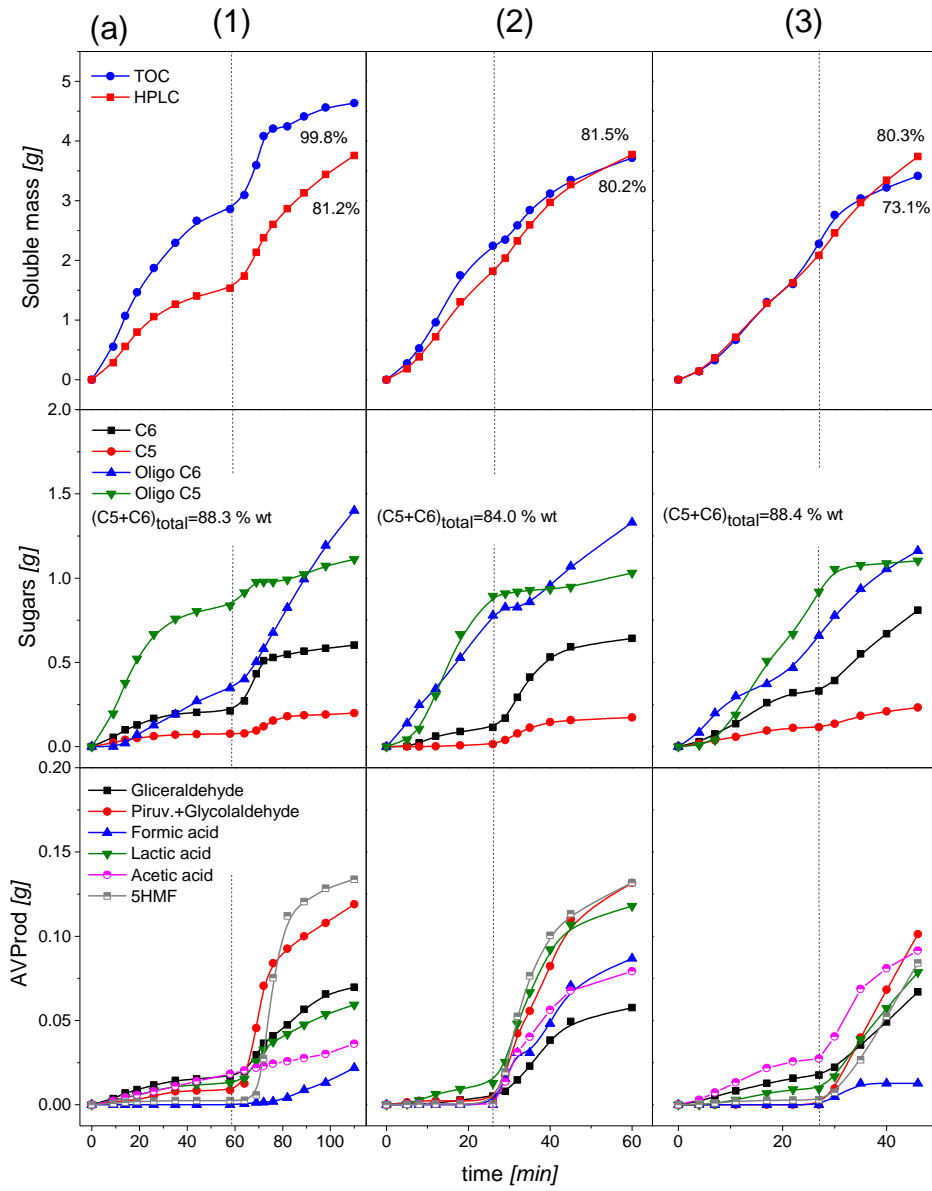
870

871

872

873

Figure 2.



874

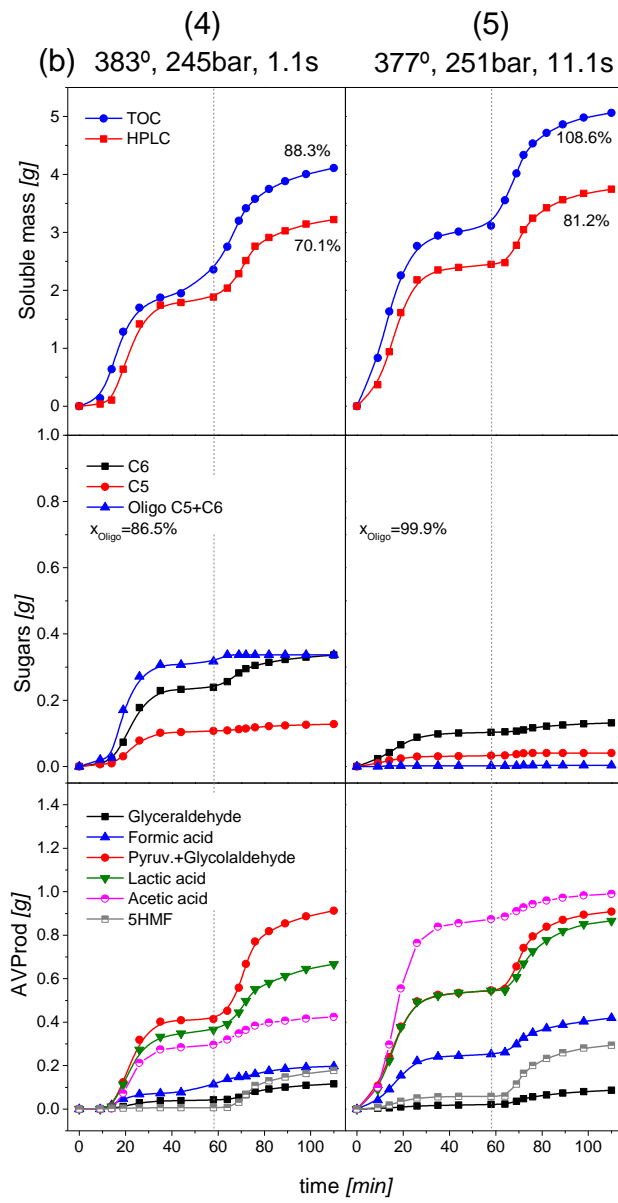
875

876

877

878

879



881

882

883

884

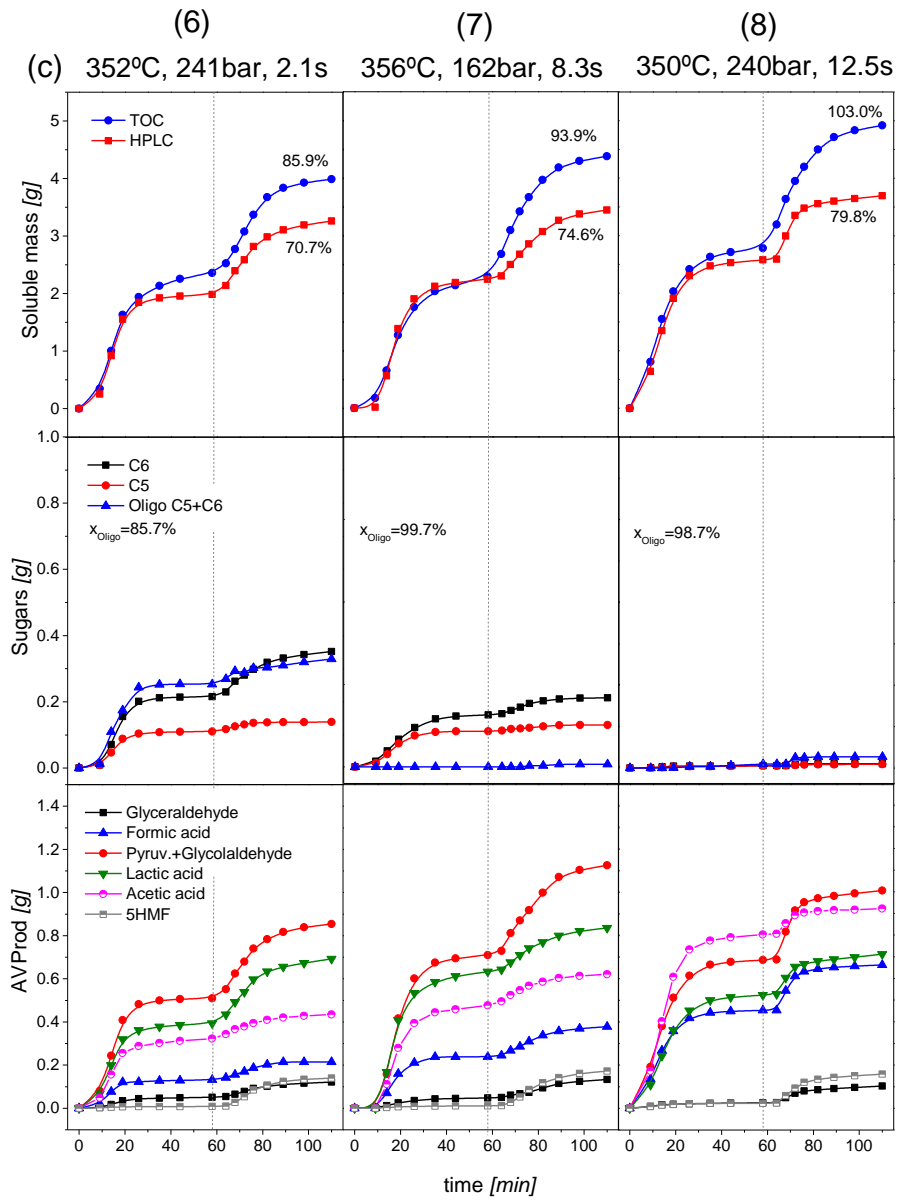
885

886

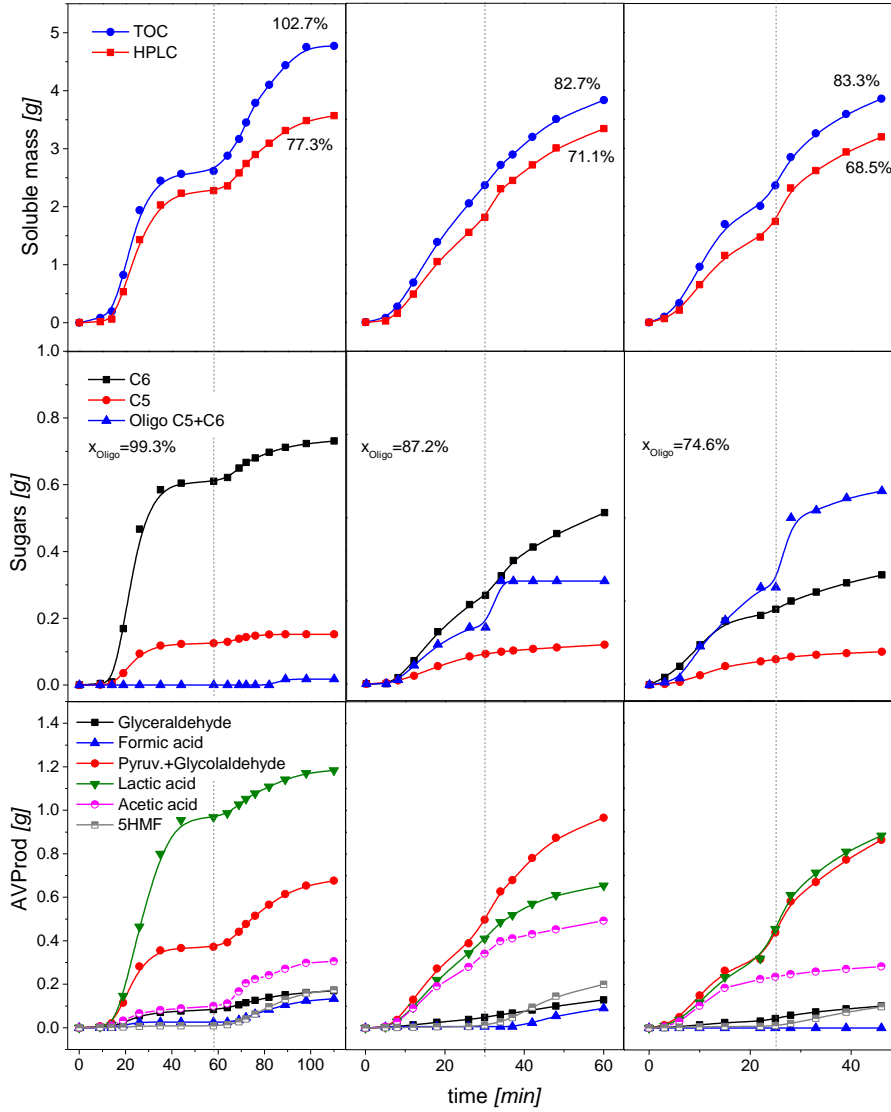
887

888

889



(9) (10) (11)
 (d) 396°C, 249bar, 0.23s 401°C, 252bar, 0.24s 398°C, 260bar, 0.24s



896
 897
 898
 899
 900
 901
 902
 903
 904
 905

906

Figure 3.

907

908

909

910

911

912

913

914

915

916

917

918

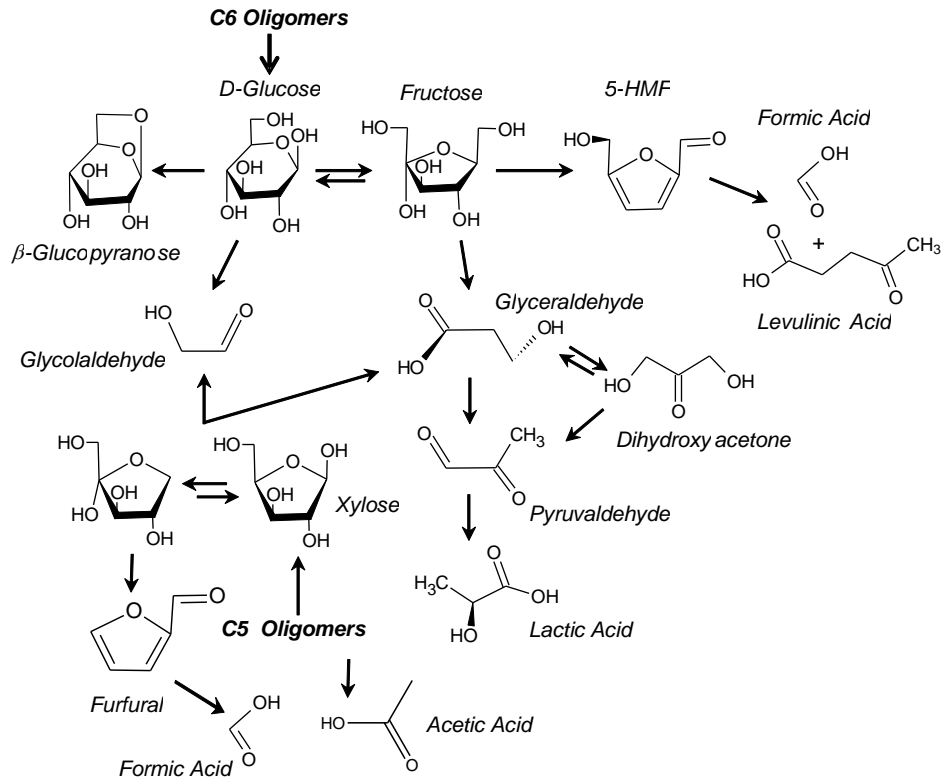
919

920

921

922

923



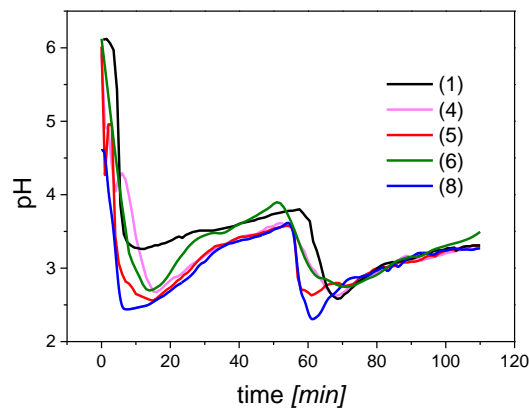
924

925

926

927

Figure 4.



924

925

926

927

928

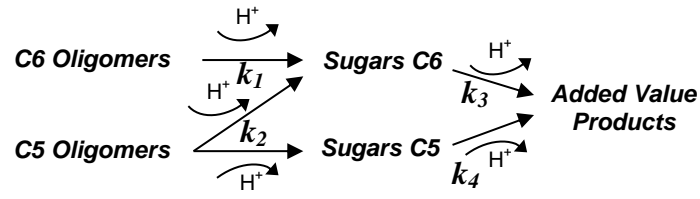
Figure 5.

929

930

931

932



933

Figure 6.

934

935

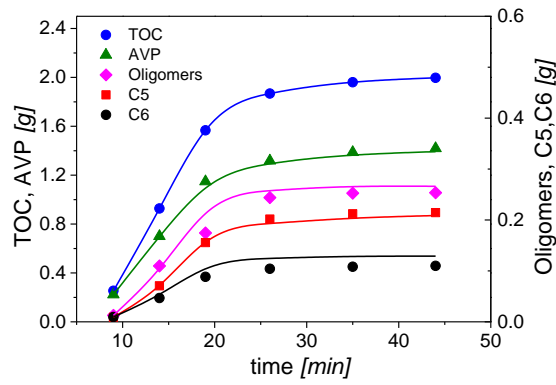
936

937

938

939

940



941

Figure 7.

942

943

944

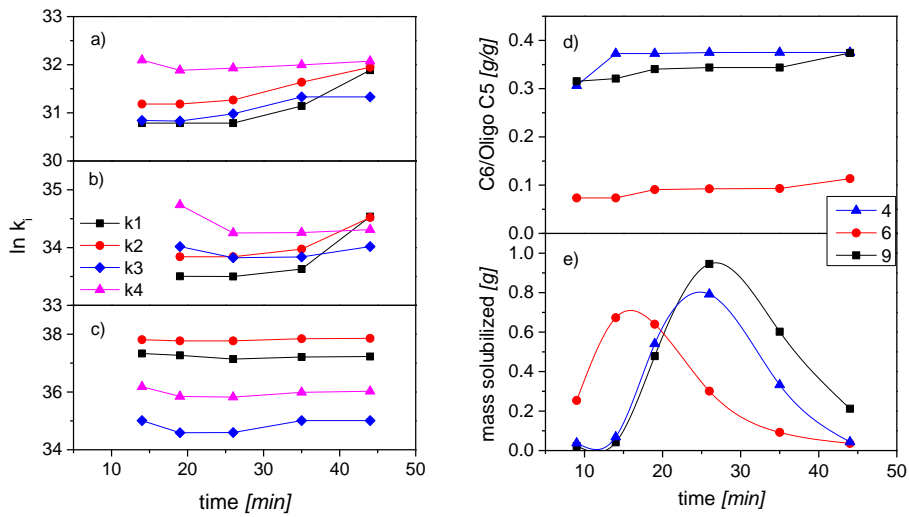
945

946

947

948

949



950

951

952

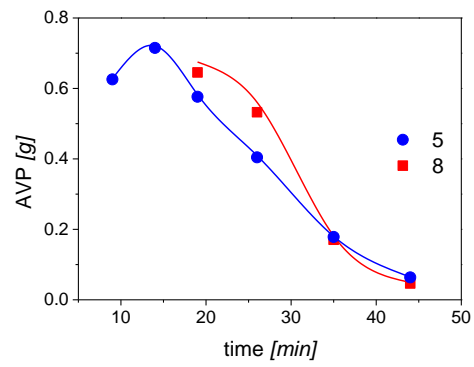
953

954

955

956

Figure 8.



957

958

959

960

961

962

963

964

965

966

967

968

969

970

971

972

973

974

975

976

977

978
979

Table 1.

Exp	T [°C]	P [bar]	t^1 [s]	Q_{SHR}^2 [cm ³ /min]	MB_{TOC}^3 [%]	$X_{Oligomers}^4$ [%]	$Y1_{AVP}^5$ -	$Y2_{AVP}^6$ -
4	383.7 ± 5.1	245.7 ± 4.6	1.06	36.0	92.2	86.5	0.008	0.079
5	377.2 ± 3.5	251.9 ± 5.9	11.15	38.5	105.9	99.9	0.247	0.281
6	352.5 ± 4.4	241.3 ± 3.7	2.10	35.2	89.3	85.7	0.004	0.109
8	349.9 ± 2.4	239.6 ± 4.2	12.50	35.8	103.1	98.7	0.233	0.132
9	396.1 ± 3.6	249.1 ± 5.1	0.23	36.8	103.6	99.3	0.440	0.254
10	401.2 ± 2.8	252.2 ± 3.9	0.24	90.1	93.0	87.2	0.481	0.278
11	398.3 ± 3.0	259.9 ± 3.4	0.24	106.2	91.2	74.6	0.530	0.228

980 ¹ t : reaction time in hydrolysis reactor, ² Flow rate in the SHR, ³ Global mass balance of the coupled process,
981 ⁴ Conversion of oligomers from hemicellulose and cellulose, ^{5,6} Yields of added value products in the time period of
982 the first and second stage of temperature during fractionation $Y_i = \text{mass}_i / \text{mass soluble material in raw biomass}$
983

984

985

Table 2.

Experiment	ADD %							
	Instantaneous				Cumulated			
	Oligomers ¹	C6 ²	C5 ³	AVP ⁴	Olig ¹	C6 ²	C5 ³	AVP ⁴
4	21.70	21.88	21.92	7.38	26.85	10.78	4.98	7.52
6	20.58	29.11	22.16	6.27	6.99	2.15	14.82	1.78
9	*	61.04	11.15	8.07	48.53	9.90	8.15	2.66
Average	21.14	37.34	18.41	7.24	27.46	7.61	9.31	3.99
5	*	*	*	5.77	*	*	*	4.94
8	*	*	*	0.93	*	*	*	1.02
Average	*	*	*	4.65	*	*	*	3.32

986 ¹ Oligomers from hemicellulose and cellulose, ² Sugars C6, ³ Sugars C5, ⁴ degradation products. * Compound not
987 detected. ADD% of total organic content was 0.0.
988
989

990

991

992

993

994

Table 3.

t_e^1 [min]	k_1^a	k_2^b	k_3^c	k_4^d
	R^2			
19	0.88	0.87	0.99	0.999
26	0.88	0.86	0.99	0.98
35	0.87	0.85	0.99	0.97
44	0.93	0.89	0.9999	0.96
Average	0.89	0.87	0.99	0.97

995 ^a Cellulose oligomer cleavage constant, ^b Hemicellulose oligomer cleavage constant, ^c Sugars C6 hydrolysis kinetic
996 constant, ^d Sugars C5 hydrolysis kinetic constant. ¹ Fractionation time.
997

998

Table 4.

k_1^a	$\ln(k)^e$	Ea/R^f [K]	k_2^b	$\ln(k)^e$	Ea/R^f [K]
A	1.04	1.03	A	1.08	1.08
B	0.04	0.06	B	0.03	0.05
C	106	46,543	C	109	48,553
k_3^c	$\ln(k)^e$	Ea/R^f [K]	k_4^d	$\ln(k)^e$	Ea/R^f [K]
A	3.26	2069	A	2.85	1834
B	22.05	24.22	B	21.25	20.15
C	1.35	4.01	C	1.70	3.58
D	87.32	35,238	D	89.63	36,081

1000
1001
1002

^a Cellulose oligomer breakup constant, ^b Hemicellulose oligomer breakup constant, ^c Sugars C6 hydrolysis constant, ^d Sugars C5 hydrolysis constant, ^e Natural logarithm of the Arrhenius' pre-exponential factor, ^f Activation energy.